

# Non-equilibrium effects in $\text{H}_2\text{--O}_2\text{--diluent}$ mixtures using the ZND reactor model

João Vargas, Karl P. Chatelain, Deanna A. Lacoste

Mechanical Engineering Program, Physical Science and Engineering Division, King Abdullah University of Science and Technology (KAUST), Thuwal 23955-6900, Saudi Arabia  
Clean Combustion Research Center (CCRC), King Abdullah University of Science and Technology

Xiangrong Huang, Rémy Mével

Center for Combustion Energy, School of Vehicle and Mobility  
State Key Laboratory of Automotive Safety and Energy, Tsinghua University, Beijing, China

## 1 Introduction

In recent years, there have been a variety of works on non-equilibrium effects on detonations [1–8]. Most of these works have been dedicated to the estimation of the cell size or width using a variety of non-equilibrium assumptions. With the advent of direct visualization of the induction zone using NO-LIF [9], characterizing possible non-equilibrium effects within the detonation cycle becomes desirable.

The objective of this work is to characterize possible non-equilibrium effects by observing the variation of the induction zone length (IZL) for thermal equilibrium and non-equilibrium thermodynamic formulations with varying initial conditions. To achieve this, the IZL was computed using a ZND reactor model for a  $\text{H}_2\text{--O}_2\text{--diluent}$  mixtures.

## 2 Methodology

Two different thermodynamic models/formulations are used to compare the IZL with and without assumptions of thermal non-equilibrium. These are the polynomial (equilibrium) and state-to-state (STS, non-equilibrium) models. The polynomial formulation is widely used in combustion applications and defined by the use of sets of coefficients of usual expressions to obtain the thermodynamical properties of known species. In this work, the NASA-9 polynomial model is used [10] with coefficients sourced from the JANAF database [11]. The STS formulation uses analytical expressions for the thermodynamics of species. Additionally, the definition of species is revised to include state-specific levels in the model. As such, individual internal levels of molecules are treated as individual pseudo-species. A more in-depth explanation of these formulations can be found in [1].

The ZND model is described by the following set of ODE [12]:

$$\frac{dY_i}{dx} = \frac{\dot{\omega}_i}{\rho u}, \quad \frac{du}{dx} = \frac{\dot{\sigma}}{1 - M^2}, \quad \frac{dP}{dx} = \rho u \frac{\dot{\sigma}}{1 - M^2}, \quad \frac{d\rho}{dx} = -\frac{\rho}{u} \frac{\dot{\sigma}}{1 - M^2} \quad (1)$$

where  $Y_i$  and  $\dot{\omega}_i$  are the mass fraction and production rate of species  $i$ . The gas velocity, Mach number, pressure, and density are denoted  $u$ ,  $M$ ,  $P$ ,  $\rho$ , respectively, and  $\dot{\sigma}$  represents the so-called thermicity which is calculated as:

$$\dot{\sigma} = \sum_i^N \left( \frac{\bar{m}}{m_i} - \frac{h_i}{C_p T} \right) \frac{\dot{\omega}_i}{\rho}. \quad (2)$$

Here, the symbols  $m_i$  and  $h_i$  represent the molar mass and the enthalpy of species  $i$ , respectively. The symbols  $\bar{m}$ ,  $C_p$  and  $T$  are the average molar mass, the specific heat at constant pressure and the temperature of the gas. The IZL is defined as the distance of the shock to the thermicity peak. In this work we mainly focus on the effect of thermal non-equilibrium dynamics on the IZL. Therefore, a straightforward comparison between simulations in this work and experimental results cannot be made. Instead, a comparison of different thermodynamic models and an assessment of the relative importance of non-equilibrium on the IZL is attempted.

### 3 Chemical-Kinetic Model

The reaction model used in this work is a reduced model from [13] and [14]. The reduced model was slightly modified to be used with state-specific species H<sub>2</sub> and O<sub>2</sub> for the case of STS simulations. Similarly to the methodology in [1], the reactive reactions of these state-to-state species must be redistributed. Only the Arsentiev [15] redistribution model was considered in this work, due to its simplicity. From the calculations in [1], the trends obtained with the other two redistribution models are expected to be similar to the ones obtained with the redistribution model of [15]. However, the second and third model presented by Vargas *et al.* should exhibit respectively a decreased and increased impact of non-equilibrium effects. The inelastic collisions of O<sub>2</sub> were used in the same manner as in [1] and are further detailed in [16, 17]. The inelastic rates for H<sub>2</sub> were adapted from calculations [18, 19] for H<sub>2</sub> + H and H<sub>2</sub> + He.

### 4 ZND Simulations and Vibrational Distributions

Figure 1 shows the comparison of the temperature (A) and thermicity (B) profiles of the Eq. (polynomial) and Non-Eq. (STS) models in a ZND reactor, for a stoichiometric mixture of H<sub>2</sub> – O<sub>2</sub> initially at 293 K and 101.3 kPa. In Fig. 1A, the Eq. temperature profile is constant within the von Neumann state (Position  $\leq 10^{-5}$  meters) and after the reaction zone (position  $> 10^{-4}$  meters), which is characterized by a sudden rise of temperature. In contrast, the Non-Eq. temperature profile shows a slow decrease of temperature in the von Neumann state and a later reaction zone onset than the Eq model. The temperature decay before the reaction zone is characterized by a change of slope around  $10^{-6}$  m, also observed on the thermicity profile evolution in Fig. 1B. The Eq. thermicity profile is constant until the reaction zone, peaks in the reaction zone at the highest energy release rate and then, relaxes to another constant value in the burnt gases. The Non-Eq. thermicity is significantly lower than the Eq thermicity profile within the induction zone. Additionally, the Non-Eq. IZL is about 1.8 times larger than the Eq. one. After the reaction zone, the evolution of the thermicity profiles are similar for both models, although the equilibrium values are slightly different.

The vibrational distribution function (VDF) can be used to assess the degree of non-equilibrium in the considered state-specific species. In Fig. 2 the VDFs of H<sub>2</sub> and O<sub>2</sub> are shown at selected positions. These positions correspond to the labels in the non-equilibrium thermicity profile in Fig. 1. Also shown in Fig. 2 are the corresponding Boltzmann distributions (i.e. the VDF under equilibrium) at the gas temperature at the corresponding position in the profile. Between the shock and position A, some excitation

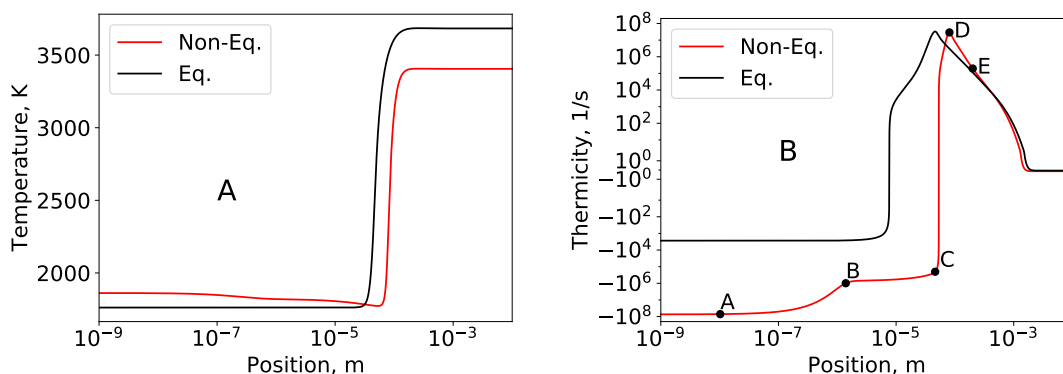


Figure 1: Temperature (A) and thermicity (B) profiles as a function of the position after the shock in a ZND reactor for a reaction model in equilibrium (black) and non-equilibrium (red). The gas is a stoichiometric mixture of  $\text{H}_2 - \text{O}_2$  initially at 293 K and atmospheric pressure.

of the  $\text{H}_2$  and  $\text{O}_2$  vibrational levels can be seen. It is also clear that the  $\text{H}_2$  excitation proceeds much faster than  $\text{O}_2$ . At position B,  $\text{H}_2$  is almost in thermal equilibrium. Between positions B and C, the same phenomena can be seen for  $\text{O}_2$ . Both species are almost in thermal equilibrium. The change of slope of the temperature decrease within the induction zone mentioned above can be attributed to the change of dominant excitation processes; before position B,  $\text{H}_2$  excitation dominates and after nearly reaching equilibrium,  $\text{O}_2$  excitation is dominant. Between positions C and D the overall reaction changes from endothermic to exothermic. This leads to a new thermal non-equilibrium zone where the distributions of  $\text{H}_2$  and  $\text{O}_2$  are far from their respective Boltzmann distribution in position D. This indicates that non-equilibrium is not limited to the induction zone, but is also taking place as a result of the main heat release event. However, thermal equilibrium is re-established fast between positions D and E.

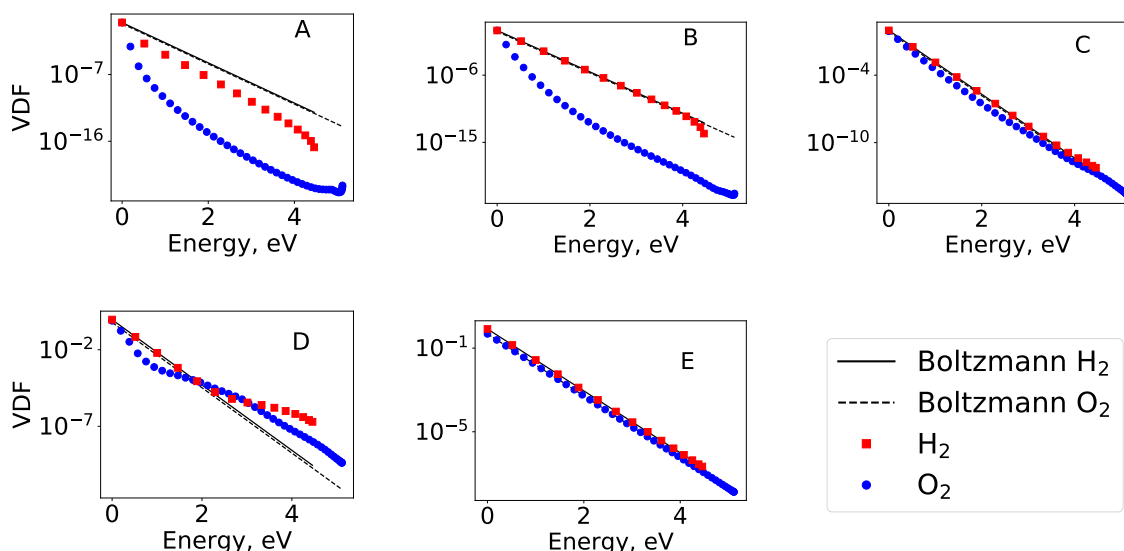


Figure 2: Vibrational distribution functions (VDF) of the considered state-specific species  $\text{H}_2$  (red) and  $\text{O}_2$  (blue) at selected locations and their respective distributions under a thermal equilibrium assumption, solid and dashed black lines, respectively.

## 5 Induction Zone Length Calculations

ZND simulations were performed using the previously validated [1] in-house code. All simulations have an initial temperature of 293 K. Figure 3 shows the IZL as a function of different initial conditions for the Eq. and Non-Eq. formulations. In the lower part of each plot, the IZL ratio between Non-Eq. and Eq. formulations is given.

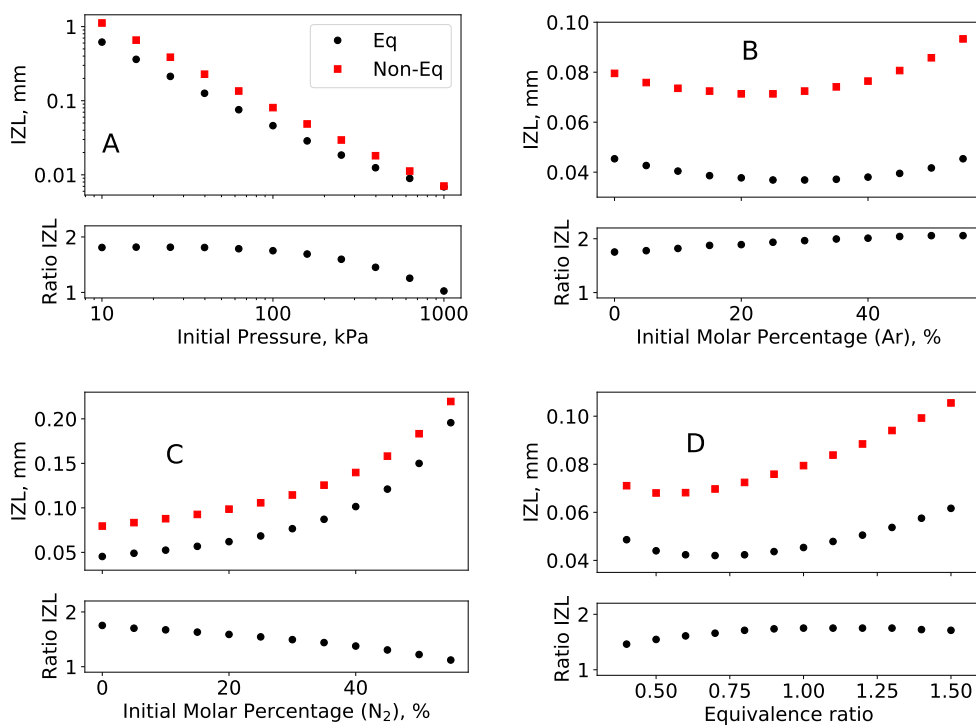


Figure 3: Induction zone length and ratio of the non-equilibrium and equilibrium IZL calculated in a ZND reactor as a function of initial pressure (A), diluent percentage of Ar (B), or  $N_2$  (C) and, equivalence ratio (D) for a  $H_2-O_2$ -diluent mixture initially at 293 K and atmospheric pressure when applicable.

### 5.1 Effect of Initial Pressure

The IZL was calculated for eleven initial pressures, between  $10^1$  and  $10^3$  kPa. Simulations were carried out for a stoichiometric mixture of  $H_2 - O_2$  initially at 293 K. The IZL as a function of the initial pressure of the gas is shown in Fig. 3A for Eq. and Non-Eq. formulations. Both models indicate a power-law decrease of the IZL with increasing initial pressure. At higher initial pressures, the Non-Eq. IZL approaches the Eq. calculated IZL. This is in line with the conventional wisdom in thermal Non-Eq. literature where the higher the rate of collisions between particles in the gas, the lower the degree of Non-Eq.

### 5.2 Effect of Diluent Percentage

The IZL was calculated for a varying Ar or  $N_2$  dilution, between 0% and 55%. The resulting mixtures of  $H_2-O_2$ -diluent were kept stoichiometric and at an initial pressure of 101.3 kPa and temperature of 293 K. The IZLs as a function of Ar or  $N_2$  dilution are shown in Fig. 3B and 3C, respectively. For Ar dilution,

both formulations predict a decreased IZL with increasing Ar percentage up to some minimum between 20–25% and 25–30% of dilution for Non-Eq. and Eq., respectively. Then, for higher dilution, the IZL increases with the diluent mole fraction. The higher the Ar dilution, the greater the difference between Eq. and Non-Eq. IZLs, as their ratio increases monotonically until it asymptotes between 50–55% dilution. In the case of  $N_2$  dilution, the IZL increases monotonically with increasing diluent percentage for both formulations. However, the ratio of the IZL decreases with increasing diluent percentage. The role of Non-Eq. in the induction zone is larger when Ar dilution is used compared with  $N_2$  as diluent.

### 5.3 Effect of Equivalence Ratio

The variation of IZL with equivalence ratio was calculated in intervals of 0.1 between 0.4 and 1.5 for mixtures of  $H_2-O_2$  with an initial pressure of 101.3 kPa and temperature of 293 K. Figure 3D shows the profile of the IZL as a function of the equivalence ratio. For lean mixtures, the IZL shows a minimum between 0.5–0.6 and around 0.7 for Non-Eq. and Eq. models, respectively. The relative importance of Non-Eq. also seems to decrease for the lean mixtures, remains constant for equivalence ratios between 1 and 1.3 and decreases slightly for richer mixtures.

## 6 Conclusions

A detailed comparison of Eq. and Non-Eq. was made in the case of a stoichiometric  $H_2 - O_2$  mixture under detonation conditions. Two zones of thermal Non-Eq. in the ZND reactor were observed, one in the induction zone and another in the vicinity of the thermicity peak. The IZL was computed in a spectrum of conditions by varying initial conditions for  $H_2 - O_2 -$  diluent mixtures. The importance of the Non-Eq. effects on the IZL was initially assessed by comparing the ratio between Non-Eq. and Eq. IZLs. Non-Eq. may have a greater or lesser impact depending on the initial conditions and its impact on IZL is up to a factor of 2.1. Based on individual parametric studies, the strongest non-equilibrium effects were observed at low pressure, high Argon dilution and rich conditions. The weakest effects were observed with nitrogen dilution or at higher pressures.

### Acknowledgments

This work has been supported by the King Abdullah University of Science and Technology through the baseline fund BAS/1/1396-01-01 and the CCF project OSR-2022-CCF-1975.49.

### References

- [1] Vargas J, Mevel R, Lino da Silva M, Lacoste DA (2022) Development of a steady detonation reactor with state-to-state thermochemical modeling. *Shock Waves* 32.
- [2] Uy KCK, Shi L, Hao J, Wen CY (2020) Linear stability analysis of one-dimensional detonation coupled with vibrational relaxation. *Physics of Fluids* 32: 12.
- [3] Uy KCK, Shi L, Wen CY (2020) Numerical analysis of the vibration-chemistry coupling effect on one-dimensional detonation stability. *Aerospace Science and Technology* 107.
- [4] Kadochnikov IN, Arsentiev IV (2020) Modelling of vibrational nonequilibrium effects on the  $H_2$ -air mixture ignition under shock wave conditions in the state-to-state and mode approximations. *Shock Waves* 30: 5.

- [5] Lin C, Luo KH (2020) Kinetic simulation of unsteady detonation with thermodynamic nonequilibrium effects. *Combustion, Explosion and Shock Waves* 56: 4.
- [6] Uy KCK, Shi LS, Wen CY (2019) Prediction of half reaction length for H<sub>2</sub>-O<sub>2</sub>-Ar detonation with an extended vibrational nonequilibrium Zel'dovich - von Neumann - Döring (ZND) model. *International Journal of Hydrogen Energy* 44: 14.
- [7] Shi L, Shen H, Zhang P, Zhang D, Wen CY (2017) Assessment of vibrational non-equilibrium effect on detonation cell size. *Combustion Science and Technology* 189: 5.
- [8] Voelkel S, Raman V, Varghese PL (2016) Effect of thermal nonequilibrium on reactions in hydrogen combustion. *Shock Waves* 26: 5.
- [9] Rojas Chavez S, Chatelain KP, Lacoste DA (2022) Induction zone length measurements by laser-induced fluorescence of nitric oxide in hydrogen-air detonations. *Proceedings of the Combustion Institute* (corrected proofs).
- [10] McBride BJ, Zehe MJ, Gordon S. (2002) NASA Glenn coefficients for calculating thermodynamic properties of individual species: National Aeronautics and Space Administration. NASA Technical Paper. <http://gltrs.grc.nasa.gov/GLTRS>
- [11] Chase M (1998) NIST-JANAF thermochemical tables, 4th Edition. American Institute of Physics
- [12] Davidenko D, Mével R, Dupré G (2009) Reduced kinetic scheme for the simulation of detonation in H<sub>2</sub>-N<sub>2</sub>O-Ar mixtures. *Proceedings of the European Combustion Meeting* 4: 6.
- [13] Baigmohammadi M, Patel V, Nagaraja S, Ramalingam A, Martinez S, Panigrahy S, Mohamed AAES, Somers KP, Burke U, Heufer KA, Pekalski A, Curran HJ (2020) Comprehensive experimental and simulation study of the ignition delay time characteristics of binary blended methane, ethane, and ethylene over a wide range of temperature, pressure, equivalence ratio, and dilution. *Energy & Fuels* 34: 7.
- [14] Nakamura H, Hasegawa S, Tezuka T (2017) Kinetic modeling of ammonia/air weak flames in a micro flow reactor with a controlled temperature profile. *Combustion and Flame* 185: 16.
- [15] Arsentiev IV, Loukhovitski BI, Starik AM (2012) Application of state-to-state approach in estimation of thermally nonequilibrium reaction rate constants in mode approximation. *Chemical Physics* 398: 1.
- [16] Lino da Silva M, Lopez B, Guerra V, Loureiro J (2012) A multiquantum state-to-state model for the fundamental states of air: the Stellar database, 5th Int. Workshop on Radiation of High Temperature Gases in Atmospheric Entry, ESA SP.
- [17] Lino da Silva, M, Guerra V, Loureiro J (2007) State-resolved dissociation rates for extremely nonequilibrium atmospheric entries. *Journal of Thermophysics and Heat Transfer* 21: 1.
- [18] Vargas J, Monge-Palacios M, Lacoste DA (2022) Quasi-classical trajectory state-specific dissociation rates of the H<sub>2</sub> + H collision. 2nd International Conference on Flight Vehicles, Aerothermodynamics and Re-entry Missions & Engineering (FAR), Heilbronn, Germany.
- [19] Vargas J, Monge-Palacios M, Lacoste DA (2022) State to state dissociation rates of H<sub>2</sub> by collision with H and He using the QCT method. 9th International Workshop on Radiation of High Temperature Gases in Atmospheric Entry, Santa Maria, Azores, Portugal.